Enhanced terahertz emission from impurity compensated GaSb

Ricardo Ascázubi,[1] Carl Shneider,[1] Ingrid Wilke,[1] Robinson Pino,[2] and Partha S. Dutta[2]
[1]*Department of Physics, Applied Physics and Astronomy, Rensselaer Polytechnic Institute, 110 8th Street, Troy, New York 12180, USA*
[2]*Department of Electrical, Computer and Systems Engineering, Rensselaer Polytechnic Institute, 110 8th Street, Troy, New York 12180, USA*
(Received 11 November 2004; revised manuscript received 3 March 2005; published 14 July 2005)

We report femtosecond optically excited terahertz (THz) emission from tellurium doped GaSb at room temperature. The influence of the majority and minority carrier type and concentrations on the strength of the THz emission is investigated. Strong enhancement of THz emission in GaSb is observed as a result of compensation of native acceptors by tellurium donors. Surface field acceleration and the photo-Dember effect are identified as THz emission mechanisms in GaSb and modeled in dependence of the majority and minority carrier type and concentrations in our GaSb samples. THz emission from *p*-type GaSb is dominated by the photo-Dember effect whereas THz emission from *n*-type GaSb is dominated by surface field acceleration. The doping conditions under which THz emission is maximized are identified.

DOI: 10.1103/PhysRevB.72.045328 PACS number(s): 78.47.+p

I. INTRODUCTION

Optical excitation of semiconductor surfaces with femtosecond (fs) titanium-sapphire (Ti:S) laser pulses is an important method to generate ultrashort terahertz (THz) radiation pulses. This type of THz radiation source has enabled the development of time domain ultrafast THz spectroscopy and THz imaging over the last decade.[1] However, important applications of these techniques in basic and applied science such as nonlinear THz-spectroscopy, nondestructive testing or biomedical imaging are still limited by the power of the available sources.[2] The development of bright, high bandwidth THz radiation sources is important in order to expand the applications of these techniques. For this purpose it is necessary to understand the THz emission process as determined by semiconductor properties.

Small band gap semiconductors are promising sources of optically excited THz radiation. One of the strongest THz surface emitters is InAs with a band gap of 0.35 eV.[3] Another recently discovered strong THz emitter is InN with a band gap of 0.7–0.8 eV.[4] Furthermore, small band gap semiconductors are attractive candidates for compact and lightweight time-domain THz spectroscopy and imaging systems powered by femtosecond fiber lasers with emission wavelengths at $\lambda \approx 1.55$ μm ($E \approx 0.8$ eV).

In previous experiments, optically excited THz emission from semiconductors was primarily investigated in dependence of experimental parameters extrinsic to the semiconductor such as excitation wavelength, excitation fluence, temperature, electric or magnetic fields.[3,5–10] Experiments which focused on the dependence of the THz emission on the doping of the semiconductor were limited to the influence of the majority carrier type.[11–13] It was observed that in small band gap semiconductors such as InAs and InSb the origin of THz emission is the photo-Dember effect[5,6,9,13,14] whereas in wide band gap semiconductors (GaAs, InP) surface field acceleration is the responsible physical mechanism.[7,8,15] Hitherto, the discrimination between the photo-Dember effect and surface-field-acceleration based THz emission has been made by analysis of the temporal wave form of the THz transient. The surface field acceleration model predicts a polarity reversal of the THz wave form if the majority carrier type changes from *p* type to *n* type whereas the photo-Dember model does not predict polarity reversal. However, the exact interplay of surface field and photo-Dember field mechanisms in THz emission from optically excited semiconductors is still under investigation.[3,4,7,8] An examination of the photo-Dember model and the surface field acceleration model reveals that in both cases the strength of the radiated THz electric field characteristically depends on the majority and minority carrier concentrations.

In this paper, optically excited THz emission from 17 high purity, selectively doped GaSb crystals is reported. GaSb is a small band gap semiconductor with a bandgap of 0.725 eV at room temperature.[16] In contrast to previous work,[11–13] we investigate the influence of the majority and minority carrier concentrations on the strength of the THz emission. We demonstrate that by systematically varying the majority and minority carrier type and carrier concentrations over three orders of magnitude the THz emission mechanism in GaSb can be tuned from being dominated by the photo-Dember effect to being dominated by surface field acceleration. We demonstrate further that within each regime photo-Dember based THz emission and surface field acceleration based THz emission are maximized under specific majority and minority carrier concentrations.

II. EXPERIMENTAL DESCRIPTION

As-grown undoped GaSb is invariably *p* type in nature due to the presence of native defects such as gallium vacancies (V_{Ga}) and gallium antisites (Ga_{Sb}).[16] In bulk GaSb crystals grown from stoichiometric melt, the net acceptor concentration is in the range of $1-2\times10^{17}$ cm^{-3}.[16] Dopants such as Te, Se, and S are commonly used to grow *n*-type GaSb crystals. The GaSb wafers used in this study were extracted from a tellurium (Te) compensated GaSb bulk crystal that was grown via the vertical Bridgman method. Details

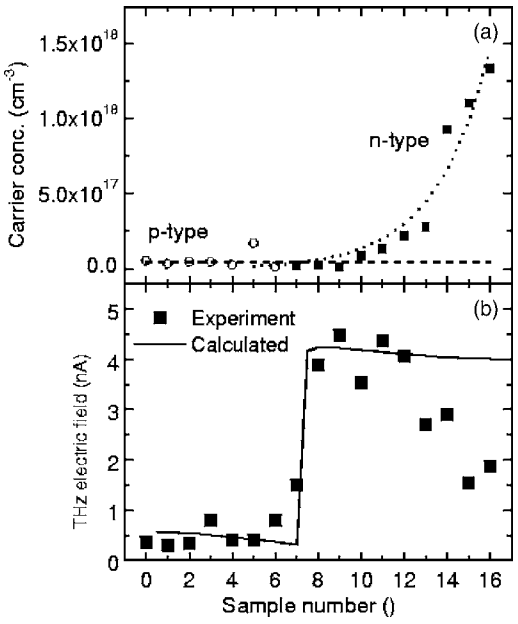

FIG. 1. (a) Electron and hole concentrations of all 17 GaSb samples. The hole concentration is 4×10^{16} cm^{-3} for all samples. The electron concentration raises exponentially with increasing Te doping. (b) Radiated THz electric field strength. Symbols are experimental data and the solid line is the calculated radiated THz field, based on the photo-Dember and surface field acceleration model.

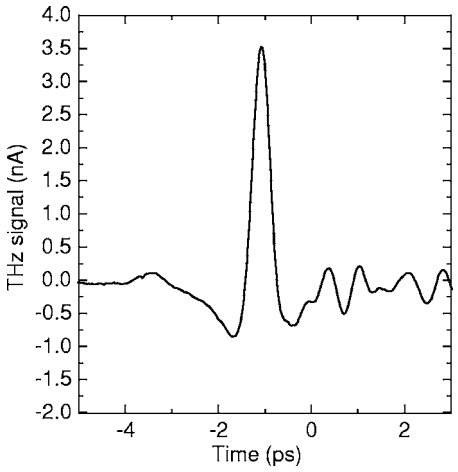

FIG. 2. Time-domain THz transient of sample No. 11. The temporal wave form exhibits the same polarity for all doping concentrations. In our analysis the peak THz emission strength is the maximum observed.

of the crystal growth experiment can be found elsewhere.[17] Considering the fact that undoped GaSb has $1-2\times10^{17}$ cm^{-3} acceptors and the segregation coefficient of Te in GaSb is 0.37, the initial Te concentration in the melt was set at 1×10^{18} cm^{-3} in order to obtain a *p*-type to *n*-type transition at approximately midway along the growth axis of the boule.[17] After the growth process, the ingots were sliced perpendicular to the growth axis to extract wafers. A total of 17 wafers were extracted from the above crystal. The wafers were lapped and polished on both sides with commercial slurries to achieve mirrorlike shining surfaces. Lapping was performed with 17.5 μm alumina slurry on a glass plate. Polishing was performed using 1 μm alumina slurry on a nylon pad and 0.1 μm alumina slurry on a velvet pad. The final wafer thickness was approximately 450 μm. Electrical characterizations were performed on all samples (0.5×0.5 cm^2 in size) using an EGK Hall Measurement System at 300 and 77 K. The ohmic contacts to the samples were provided by indium annealed at 500 °C for 1–2 min. The samples used in our measurements were taken from the region of the 2 in. diameter wafer lying halfway between the center and the edge along the radial direction. The measured net carrier concentration and the type of the wafers extracted along the growth direction are shown in Fig. 1(a). In the first seven wafers (0–6), the Te level is lower than the native acceptor concentration and, hence, they are *p* type. The wafers (7–16) have higher Te concentration than the native acceptor concentration and hence they are *n* type. It is worth pointing out that in undoped crystals, the native acceptor concentration remains same along the entire length of the boule.

The Te-doped GaSb samples were subject to ultrafast optical excitation by a Ti:sapphire laser. Pulses of 70 fs duration, with a central wavelength of 800 nm and a repetition rate of 82 MHz were used in a pump-probe arrangement.[12] The energy of the pump beam was 7 nJ per pulse. The pump beam was slightly focused by a lens ($f=50$ mm) on the GaSb sample. The angle of incidence of the optical pump beam onto the GaSb samples was 45°. The polarization of the pump beam was parallel to the plane of incidence. The THz electromagnetic transient was collected and steered to the electro-optic detector by four off-axis parabolic mirrors and was finally measured by electro-optic detection using a 1 mm thick ⟨110⟩ ZnTe crystal. The single-diode current in this experiment was 270 μA. Under these conditions, a *p*-type ($\approx1\times10^{16}$ cm^{-3}) InAs sample gave a peak THz signal of ≈25 nA.

III. DISCUSSION

In our THz emission experiments we have observed strong optically excited THz radiation from all 17 GaSb samples. The temporal wave form of the THz transient exhibits the same polarity for all doping concentrations. The THz transient emitted by sample No. 11 is displayed as an example in Fig. 2. The THz emission strength depends strongly on the electron and hole concentrations as illustrated in Fig. 1(b). In this figure, the peak THz emission is plotted as a function of the sample number which in turn defines the doping concentration. We observe that the THz emission for the *n*-type samples Nos. 7–16 is stronger than that of the *p*-type samples (Nos. 0–6). The strongest THz emission is obtained from highly compensated ($n_b\approx p_b$) GaSb samples. The *n*-type samples showed a significant enhancement after repolishing the GaSb surface. This strong dependence of the THz emission on the surface morphology was not observed for the *p*-type samples.

In order to explain our experimental observations we study the transport of carriers in the ultrafast regime.

We have not observed a dependence of the strength of the THz emission on the angle between the polarization of the excitation laser beam and the crystallographic orientation of the GaSb surface. For this reason we have not regarded optical rectification as a possible mechanism of THz radiation. Further, the optical absorption length in GaSb at the excitation wavelength (800 nm) is short ($d \approx 250$ nm),[18] while the required coherence length[19,20] is expected on the order of the THz wavelength. Therefore, our analysis is focused on two contributions; the acceleration of carriers by the surface depletion/accumulation field[12] and the photo-Dember effect.[13,14] The surface field model explains THz emission through acceleration of photocarriers by a surface depletion or acceleration field present in the vicinity of the semiconductor surface. The origin of the surface field is band bending due to the Fermi level pinning by surface electronic states. The photo-Dember effect is observed at the surface of semiconductors after photoexcitation. A photo-Dember field occurs as the result of different diffusion coefficients of electrons and holes.

In our analysis we calculate the strength of the emitted THz radiation field as a function of the electron and hole concentrations. The strength of the emitted THz field is determined by the time derivative of the drift and diffusion currents in our photoexcited GaSb samples. The discussion begins with the photo-Dember effect. Drift and diffusion currents of electrons j_n and holes j_p in an illuminated semiconductor are described by the following equations:

$$J_n = eE(\mu_n n_b + \mu_n \Delta n) + \mu_n k_B T \frac{\partial n_b}{\partial z} + \mu_n k_B T \frac{\partial \Delta n}{\partial z}, \quad (1)$$

$$J_p = eE(\mu_p p_b + \mu_p \Delta p) - \mu_p k_B T \frac{\partial p_b}{\partial z} - \mu_p k_B T \frac{\partial \Delta p}{\partial z}. \quad (2)$$

According to the Dember hypothesis[7,21] an electric field arises in the illuminated semiconductor such that

$$J_{total} = J_{\Delta p} + J_{\Delta n} = 0. \quad (3)$$

From this condition the photo-Dember field E_D is obtained

$$E_D = \frac{k_B T_e}{e} \frac{b \frac{\partial \Delta n}{\partial z}}{p_b + n_b b + \Delta n(1+b)}, \quad (4)$$

where $b = \mu_n / \mu_p$ is the ratio of mobilities of electrons and holes, Δn is the photocarrier concentration, T_e is the carrier temperature obtained from the residual photon energy, and p_b and n_b are the bulk electron and hole concentrations. The photo-Dember field is derived under the assumptions that the excess energy from the laser photons is transferred to the electrons, that the number of photoexcited electrons Δn is equal to the number of photoexcited holes Δp and that $\partial p_b / \partial z$ and $\partial n_b / \partial z$ are negligible. The direction of the surface normal is chosen as the z axis of our coordinate system. Electromagnetic radiation in the far field arises from the photocurrent as

$$E_{far} = \frac{S}{4\pi\epsilon_0 c^2 \tau} \int_0^{Bulk} J(z) dz \left(\frac{1}{r}\right) T_1. \quad (5)$$

In Eq. (5), S is the laser focal spot size, c is the velocity of light, ϵ_0 is the permitivity of vacuum, and τ is the duration of the laser pulse. $J(z)$ is the photocurrent obtained from Eqs. (2) and (1). T_1 is a dimensionless time envelope defined as: $T_1 \equiv 2 \exp\{-[(t - r/c)/\tau]^2\}$ $(t/\tau - r/\tau c)$. The relationship between the magnitude of the radiated electric field and the electron and hole concentrations in GaSb is obtained by integrating Eq. (5) and results in

$$E_{far} = \frac{S}{4\pi\epsilon_0 c^2 \tau r} \frac{k_B T_e \mu_n}{(1+b)} \left\{ \frac{b(n_b - p_b)}{1+b} \times \ln\left[1 + \frac{\Delta\tilde{n}(1+b)}{p_b + b n_b}\right] - \Delta\tilde{n} \right\}, \quad (6)$$

where the number of photoexcited carriers may be estimated as $\Delta n = \Delta\tilde{n} e^{-\alpha z}$. Next, we consider THz emission due to surface field acceleration. The surface field E_s across the depletion region is assumed to be homogeneous

$$E_S = \frac{e n_{eff}}{\epsilon_r \epsilon_0}(W - z) \quad : 0 < z < W$$

$$= 0 \quad : W < z, \quad (7)$$

where n_{eff} is the "effective" carrier density assuming total compensation of both carriers: $n_{eff} = |p_b - n_b|$. The depletion width W is calculated from the surface potential due to band bending[22]

$$W = \sqrt{\frac{2\epsilon_r \epsilon_0 (V_s - k_B T/e)}{e|p_b - n_b|}}. \quad (8)$$

The induced photocurrent is

$$J_{n,p} = e \mu_{n,p} \Delta\tilde{n} e^{-\alpha z} E_s(z). \quad (9)$$

With Eqs. (5), (7), and (9) we obtain the relationship between THz emission due to surface field acceleration and electron and hole concentrations in GaSb:

$$E_{far} = \frac{S e^2 \mu_{n,p} \Delta\tilde{n}}{4\pi\epsilon_0^2 \epsilon_r c^2 \tau r \alpha^2} |p_b - n_b| [e^{-\alpha W} + W\alpha - 1]. \quad (10)$$

Before we discuss the THz emission in dependence of electron and hole concentrations we first consider how the surface field and photo-Dember field change with the electron and hole concentrations. For this purpose, we have calculated the surface acceleration field and the photo-Dember field according to Eqs. (4) and (7) for GaSb and our range of doping concentrations.

We assume that the electron and hole mobilities of GaSb are $\mu_e = 5000$ cm^2/Vs and $\mu_h = 850$ cm^2/Vs.[23] Carrier scattering in our samples will occur on different time scales. Relevant to THz emission are scattering events on a subpicosecond time scale. Further scattering events occurring on longer time scales will result in lower mobility values. The dominant scattering mechanisms in GaSb in this time scale are intervalley scattering and optical phonon emission.[24]

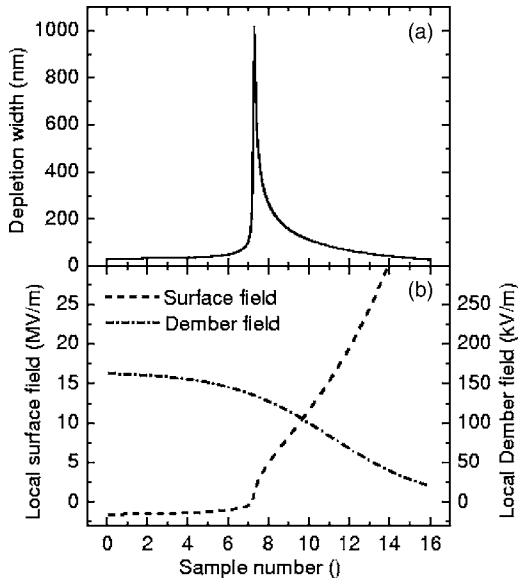

FIG. 3. (a) Calculated carrier depletion width. The surface field arises across the depletion width, while the Dember field is independent on this width. (b) Calculated surface and photo-Dember local electric fields.

In our experiment the native p-type concentration is assumed to be 4.4×10^{16} cm^{-3} and the Te concentration is assumed to follow $[\mathrm{Te}]=2.5\times10^{15}\exp(x/2.51)$ cm^{-3}, where x is given in millimeters. Sample 0 corresponds to $x=0$ and sample 16 correspond to $x=16$. The depletion width W is calculated for all doping concentrations in our GaSb samples assuming surface potentials due to band bending of $V_s=0.65$ eV for n type and $V_s=0.05$ eV for p-type GaSb,[22] and a dielectric constant[16] $\epsilon_s=15.7$. The induced photocarrier concentration is estimated to be $\Delta\tilde{n}\approx1.4\times10^{17}$ cm^{-3}. The results of the electric field calculations are illustrated in Fig. 3(b). In addition to the gradient of photocarrier concentration $\partial\Delta n/\partial z$, the photo-Dember field depends on the bulk electron and hole concentrations and mobilities. The photo-Dember field is always positive and stronger in the p-type samples than in the n-type samples. The surface field is negative for the p-type samples and positive for the n-type GaSb samples. For n-type samples the surface field E_s is much stronger than the photo-Dember field E_D. This is because $E_s\propto\sqrt{n_{eff}}$ and because the band bending for n-type GaSb is much stronger than for p-type GaSb. The depletion width W of our samples is maximized for highly compensated GaSb.

Next, we have calculated the strength of the emitted THz-radiation field according to Eqs. (6) and (10) for GaSb and our range of doping concentrations. The results of this calculation are compared to our experimental data and illustrated in Fig. 1(b). Our calculations are performed with an electron temperature of $2/(3k_B)(h\nu-E_g)$ in order to reflect the relative magnitude of the THz emission from the p-type and n-type samples.

In previous work the hot carrier temperature was estimated to be $T_e\approx2/(3k_B)(h\nu-E_g)$ for GaAs excited by 3.1 eV laser radiation at room temperature[7] and $T_e\approx1/(2k_B)(h\nu-E_g)$ for InP excited by 1.5 eV laser radiation at 10 K.[8] Recombination events are not expected in this ultrafast regime[25] but the excitation energy is larger than the intervalley scattering threshold[24] and phonon emission scattering times are expected to be around 200 fs in this doping range. We attribute the decreased electron temperature required to fit our data to these phenomena.

The surface field model predicts the highest THz emission for a compensated semiconductor where $p_b\approx n_b$. Data from Fig. 1(b) confirms this as the most prominent enhancement of THz emission in GaSb. THz emission is maximized in highly compensated GaSb because under this condition the depletion width W is maximized, and wider than the optical absorption length. Based on this comparison we conclude that in p-type GaSb THz emission is dominated by the photo-Dember effect while surface acceleration is responsible for THz emission in highly compensated and in n-type GaSb.

This interpretation is also supported by the following experimental observations: The polarity of the time-domain THz transient does not change for our samples when the majority carrier type change from p to n. This is in agreement with our calculations showing that in the p-type samples the contribution to THz emission by the photo-Dember field is stronger than the THz emission due to surface field acceleration. Moreover, we observed that the n-type samples showed a significant enhancement of THz emission after repolishing the GaSb surface. This strong surface morphology dependence of THz emission is not observed in the p-type samples. This is also in agreement with the recent observation that surface treatment of GaSb enhances the surface field and as a result THz emission.[26] In contrast the photo-Dember effect is known to be rather insensitive to mechanical polishing of the surface.[27] These observations corroborate our interpretation that surface field acceleration dominates in the compensated and n-type GaSb samples while the photo-Dember effects is the origin of THz emission in the p-type samples.

We observe in our experiments that THz emission from GaSb samples, where $n_b\gg\Delta\tilde{n}$, is lower than that of highly compensated samples. The decrease of THz emission with increasing n-type doping occurs for bulk carrier concentrations equal or larger than the density of photoexcited carriers. This decrease of THz emission with increasing n-type doping can not be explained by the surface field model. We assume that the THz emission decreases for bulk electron densities larger than the photocarrier density due to increased electron-electron scattering. This assumption is supported by the observation that the mobility of the electrons decreases with increasing carrier concentration in this range.[28] Also, we observe a local peak in THz emission (sample No. 3) for the range of GaSb samples where the photo-Dember effect dominates THz emission. For this sample the bulk carrier concentrations are found to be $\mu_n n_b\approx\mu_p p_b$.

We also analyzed the frequency spectra of the THz transients. In Fig. 4 the normalized Fourier amplitudes for $f=0.25$ THz, $f=0.7$ THz, and $f=1.5$ THz are illustrated as a function of the carrier concentration. We observe that the n-type GaSb samples exhibit a larger THz bandwidth than the p-type GaSb samples. Although the strength of THz emission decreases for bulk electron concentrations n_b larger

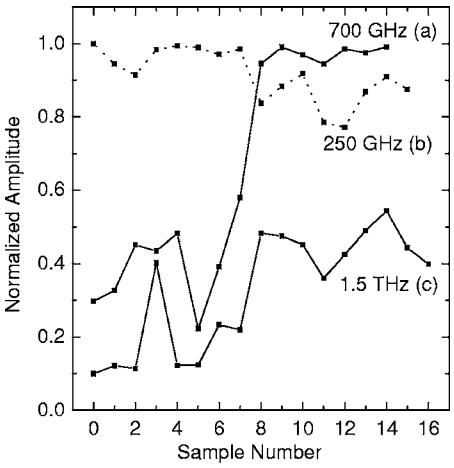

FIG. 4. Normalized fast Fourier transform spectral contributions. Sample Nos. 0–7 are *p* type and sample Nos. 8–16 are *n* type.

than $\Delta\tilde{n}$, the bandwidth of the radiation does not change for this range of carrier concentrations. THz emission dominated by surface field acceleration has a larger bandwidth than THz emission dominated by the photo-Dember effect.

IV. CONCLUSIONS

We have investigated THz radiation from a set of GaSb samples with a broad range of electron and hole concentrations. The THz emission is strongly dependent on the doping concentrations. The surface field dominates in the highly compensated region (where $p_b \approx n_b$) due to a wide depletion layer and higher surface potential in the *n*-type samples. In the region where $\Delta\tilde{n} \ll n_b$, THz emission decreases, however, the bandwidth of the THz radiation is preserved.

It has been demonstrated that THz emission in GaSb can be enhanced by more than an order of magnitude using high purity semiconductor crystal growth and selective doping techniques. The strength of THz emission in dependence of the majority and minority carrier concentrations agrees well with theoretical predictions. These results suggest a re-examination and possible revision of the relative THz emission strengths of different III–V semiconductors as reported previously.

ACKNOWLEDGMENTS

R.P. would like to acknowledge the National Science Foundation for support. This research was supported in part by the Office of Naval Research under Contract No. N00014-02-1-0458. The authors would like to thank Youngok Ko for assistance in the Hall measurements of the samples used in this work.

[1] D. Mittleman, *Sensing with Terahertz Radiation* (Springer-Verlag, New York, 2003).
[2] R. Woodward, V. Wallace, D. Arone, E. Linfield, and M. Pepper, J. Biol. Phys. **29**, 257 (2003).
[3] H. Takahashi, A. Quema, R. Yoshioka, S. Ono, and N. Sarakura, Appl. Phys. Lett. **83**, 1068 (2003).
[4] R. Ascázubi, I. Wilke, K. Denniston, H. Lu, and W. J. Schaff, Appl. Phys. Lett. **84**, 4810 (2004).
[5] S. Kono, P. Gu, M. Tani, and K. Sakai, Appl. Phys. B: Lasers Opt. **B71**, 901 (2000).
[6] S. Howells, S. Herrera, and L. Schlie, Appl. Phys. Lett. **65**, 2946 (1994).
[7] J. Heyman, N. Coates, A. Reinhardt, and G. Strasser, Appl. Phys. Lett. **83**, 5476 (2003).
[8] M. Nakajima, M. Hangyo, M. Ohta, and H. Miyazaki, Phys. Rev. B **67**, 195308 (2003).
[9] J. Heyman, P. Neocleous, D. Herbert, P. Crowell, T. Mueller, and K. Unterrainer, Phys. Rev. B **64**, 085202 (2001).
[10] M. Hasselbeck, D. Stalnaker, L. Schilie, T. Rotter, A. Stintz, and M. Sheik-Bahae, Phys. Rev. B **65**, 233203 (2002).
[11] M. Johnston, D. Whittaker, A. Corchia, A. Davies, and E. Linfield, Phys. Rev. B **65**, 165301 (2002).
[12] X.-C. Zhang and D. Auston, J. Appl. Phys. **71**, 326 (1992).
[13] P. Gu, M. Tani, S. Kono, K. Sakai, and X.-C. Zhang, J. Appl. Phys. **91**, 5533 (2002).
[14] T. Dekorsy, H. Auer, H. Bakker, H. Roskos, and H. Kurz, Phys. Rev. B **53**, 4005 (1996).
[15] X.-C. Zhang, B. Hu, J. Darrow, and D. Auston, Appl. Phys. Lett. **56**, 1011 (1990).
[16] P. Dutta, H. Bhat, and V. Kumar, J. Appl. Phys. **81**, 5821 (1997).
[17] R. Pino, Y. Ko, and P. Dutta, J. Electron. Mater. **33**, 1012 (2004).
[18] S. Adachi, J. Appl. Phys. **66**, 6030 (1989).
[19] A. Nahata, D. Auston, T. Heinz, and C. Wu, Appl. Phys. Lett. **68**, 150 (1996).
[20] M. Nagai, K. Tanaka, H. Ohtake, T. Bessho, T. Sugiura, T. Hirosumi, and M. Yoshida, Appl. Phys. Lett. **85**, 3974 (2004).
[21] W. Mönch, *Semiconductor Surfaces and Interfaces* (Springer, New York, 2001).
[22] K. Schirm, P. Soukiassian, P. Mangat, and L. Soonckindt, Phys. Rev. B **49**, 5490 (1994).
[23] S. Sze, *Physics of Semiconductor Devices* (Wiley, New York, 1991).
[24] W. Pelouch and L. Schlie, Appl. Phys. Lett. **66**, 82 (1995).
[25] A. Titkov, E. Iluridze, I. Mironov, and V. Chaban, Sov. Phys. Semicond. **20**, 25 (1986).
[26] S. Winnerl, S. Sinning, T. Dekorsy, and M. Helm, Appl. Phys. Lett. **85**, 3092 (2004).
[27] S. Los and M. Nowak, Electron Technol. **29**, 45 (1996).
[28] R. Pino, Y. Ko, and P. Dutta, J. Appl. Phys. **96**, 1064 (2004).